Plasma Chemistry and Plasma Processing, Vol. 16, No. 1, 1996 (Supplement)

CHARACTERIZATION OF D.C. PLASMA TORCH VOLTAGE FLUCTUATIONS

J.F. COUDERT, M.P. PLANCHE, P. FAUCHAIS

L.M.C.T.S. - Equipe "Plasma, Laser, Matériaux" Université de Limoges - URA CNRS 320 - Faculté des Sciences 123, av. A. Thomas - 87060 Limoges Cedex - FRANCE

The arc root fluctuations at the anode-nozzle of a d.c. plasma spray torch with a special configuration of the electrodes allowing to work with the same gas flowrate with nozzle diameters ranging from 6 to 10 mm were systematically studied. The plasma gas was Ar/H2 (25 vol % H2), the current was varied between 200 and 600 A and the plasma gas flowrate between 24 and 80 slm. After 30-60 mn working the nozzle wall started to be sufficiently eroded to have a stagnant arc spot which lived until arcing created another one. It was shown that the life time of the upstream arc spots were 30-40 % longer than the downstream ones which could play an important role in the electrode erosion. Dimensional analysis allowed to find a relationship between the nozzle diameter D, the arc current I and gas flow rate G and the mean spot lifetime which is closely connected with the difference between D and the electrical diameter of the arc column. The comparison of voltage signal and light emission at a point of the plasma jet close to the nozzle exit on its axis allowed to determine the mean electrical field within the plasma column and the mean position of the arc root. The comparison with the electrode erosion area for well defined conditions showed a good correlation with the calculated arc root position.

0272-4324/96/0300-211S$09.50/0

NOTATIONS

E : Electric field.
$_b$: Breakdown field.
τ : Spot lifetime.
σ : Voltage jump amplitude.
θ : Time of flight of the plasma bubble from the place where the arc restriked to the optical axis position.
D : Nozzle diameter.
e : Thickness of the cold layer.
G : Gas flowrate
I : Current intensity.
L : Distance between the cathode tip and the the optical axis.
l : Length of the arc column.
U_a : Anode fall.
U_c : Cathode fall.
V_g : Voltage between the column and the anode wall.
V_l : Voltage drop along the arc loop.
V_m : Voltage minimum.
v : Flow velocity.
v_b : Voltage breakdown.
D : "Downstream" restriking.
U : "Upstream" restriking.

1. INTRODUCTION

Although electric arcs have been extensively studied for many years for their material applications, the electrode regions are still poorly understood. This lack of informations, due to the complexity of the phenomena which take place and to the difficulty of modelling, has stimulated many research works. Nevertheless, the most refined experimental works or modellings were dealing with low power level transferred arcs with a high stability and a well defined axisymetric geometry. The blown and thermally constricted arcs, such as those encountered in torches used for plasma spraying, were experimentally studied in a less detailed way, namely because of the presence of a solid nozzle prevented to directly observe the arc. Different theoritical models were proposed in the past for the arc column [1,2,8] based on more or less

restrictive asumptions and where the time instabilities as well the real shape of the arc were ignored. But in a classical configurated plasma spray torch, if the arc geometry is rather simple in the vicinity of the cathode tip, the arc exhibits a complex and unstable shape in the arc-anode attachment region. The superimposed flow and the magnetic forces influence the arc-anode attachment column which is continuously distorted.

These deformations and the breakdown phenomena which occur through the cold layer surrounding the arc, generate highly transient variations in the arc voltage and, consequently, strong fluctuations in the plasma flow, namely concerning the temperature and the velocity field.

Even though these arc instabilities were already observed in the past, there is only a little amount of work devoted to their specific study [3,4,5].

In this context, it appears necessary to define some important features of the arc dynamic and to correlate their characteristics with the operating parameters. This is the object of the experimental work presented below, where a special attention was paid to the study of the arc voltage transient evolution of a classically designed plasma spray torch.

2. SUGGESTED ARC BEHAVIOR

The plasma was generated with a torch equipped with a thoriated tungsten stick type cathode, coaxial with the cylindrical channel of the anode-nozzle in which the arc was thermally constricted. The gas was axially injected along the cathode tip conically shaped with a 60° angle. The arc column exhibiting an axisymetric shape close to the cathode tip, was surrounded by a cold and electrically insulating gas layer.

The connection with the anode wall was realized by a plasma loop crossing the cold flow and submitted to a drag force [6]. Due to the thermal pinch, the connecting arc loop was severly constricted in the nozzle-wall vicinity which gave rise to an anodic spot through which flowed an important heat flux ($>10^9$ W/m^2).

The thermal pinch was responsible for the current lines curvature in the contraction zone from which an anodic jet was created by the magnetic body forces [7]. The combination of the anodic jet and of the main flow contributed to the distortion of the arc loop which was gradually lengthened downstream of the spot location and towards the opposite wall (see fig 1-b). The behavior of the anodic spot during the lengthening of the arc seemed to depend on the surface roughness. In the case of a smooth

channel e.g. for a new nozzle, the spot was sliding continuously in the flow direction until a breakdown occured giving rise to an "upstream" new spot (see fig 1-c). In the case of a "sliding" mode, the nozzle showed a very weak erosion, almost without surface modification as confirmed by examination of the channel after each run (during about 30 mn). As soon as erosion took place the surface roughness changed with the occurence of defects in the channel where the arc root was anchored during a given stagnation time. This stagnation time, or spot lifetime, was limited by the occurence of a new spot due to another breakdown through the cold layer. Starting with a new nozzle and operating the torch with a given set of working parameters it was observed that during the first ten hours of work the behavior progressively shifted from the sliding mode to the stagnation mode, for which the mean residence time of the spot plays a crucial role for the nozzle erosion.

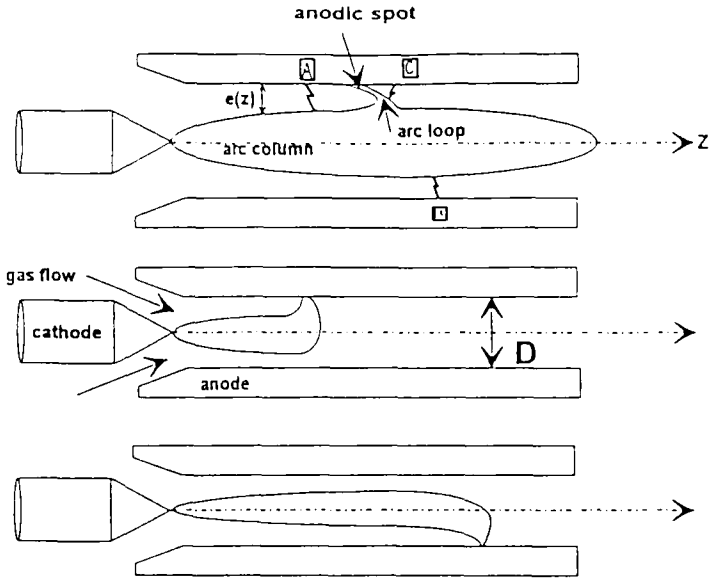

Figure 1 : a-Schematic configuration of the arc at the end of a lengthening phase
b-After an upstream restriking.
c-After a downstream restriking.

This was suggested by the morphology evolution of the wear traces left in the nozzle channel, where the stagnation is characterized by a severe and rather well located erosion.

3. ARC EROSION VOLTAGE EVOLUTION

In the following, it will be assumed that the stagnation mode dominates with the eventuality of both upstream rearcings (A in fig 1-a) and downstream rearcings (B or C in fig 1-a).

Each time a breakdown occured, a new spot was created by rearcing associated with a sudden decay of the arc voltage (20-40V in less than 10μs). At the end of the decay, the voltage showed a local minimum value from which an almost linear increase took place, associated with the arc column stretching which was limited by the occurence of another breakdown and its corresponding voltage jump. The resulting temporal evolution of the arc voltage is typically represented by a saw-tooth shaped waveform as shown in fig 2. The signal was recorded for an Ar/H2 (45/15 slm) plasma with a 10μs/pt sampling rate. The time between two consecutive jumps defined the stagnation time or the spot lifetime. At the beginning of a stretching phase only the arc column was lengthened in contrast with the final situation where both the column and the arc loop were lengthened, leading to an increase of the ramp slope. It was observed that this modification of the slope was more pronounced in the case of low arc currents and large nozzle diameters (typically 200A, $\Phi \geq 8mm$) than in the opposite case (600A, $\phi = 6mm$) where the voltage ramps were linear, with an almost constant slope.

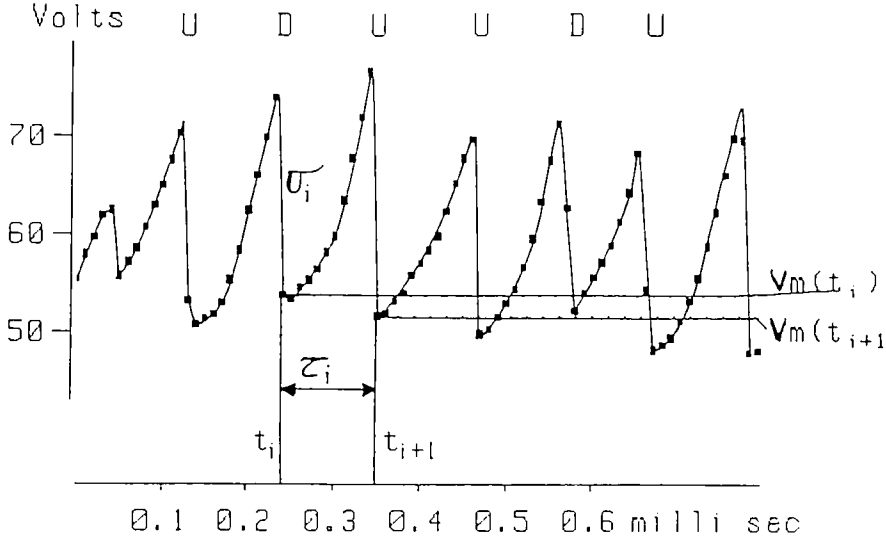

Figure 2 : Resulting temporal evolution of the arc voltage.

The time, 2ε, required for a rearcing to take place was less than $10\mu s$, which was the time step used for the voltage sampling. For this reason, the voltage decay associated with each rearcing must be considered as a mathematical discontinuity in the voltage waveform, and will be referred as a "jump".

Referring to figure 2, the following quantities can be defined :

t_i : time of occurence of the i^{th} jump associated with the i^{th} anodic spot.

$\tau_i = t_{i+1} - t_i$, i^{th} spot lifetime

$V_m(t_i)$: local minimum of the voltage

σ_i : voltage jump amplitude

U for "Upstream" restriking with $V_m(t_i) < V_m(t_{i-1})$

D for "Downstream" restriking with $V_m(t_i) > V_m(t_{i-1})$

The arc voltage V(t) is the sum of the cathode and anode falls, respectively U_a and U_c, of the voltage drop along the arc column $V_c(Z_{i-1})$ which depends on the actual spot location Z_{i-} and of the voltage drop along the arc loop, $V_l(t)$, which depends on time because of length variation of the loop (fig 3).

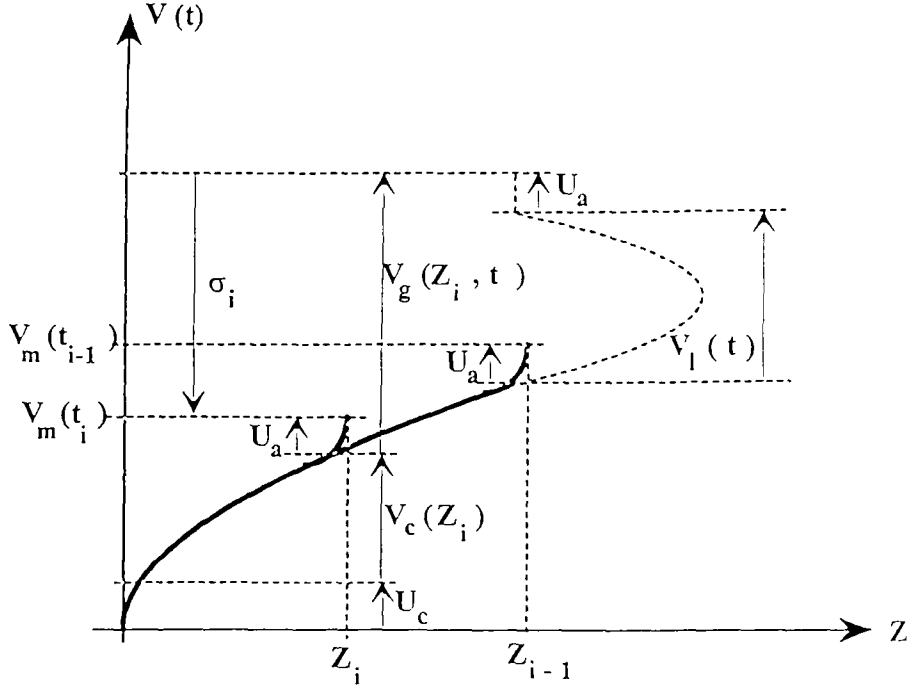

Figure 3 : Arc voltage evolution

It comes for the arc voltage :

$$V(t) = U_c + U_a + V_c(Z_{i-1}) + V_l(t) \qquad t_{i-1} < t < t_i \qquad (1)$$

Just after a spot creation, at time $t_{i-1} + \varepsilon$, the voltage is :

$$V(t_{i-1} + \varepsilon) = V_m(t_{i-1}) = U_c + U_a + V_c(Z_{i-1}) \qquad (2)$$

and just before the further breakdown giving rise to the new spot location, Z_i, at time $t_{i-1} + \tau_{i-1} - \varepsilon = t_i - \varepsilon$

$$V(t_i - \varepsilon) = U_c + U_a + V_c(Z_{i-1}) + V_l(t_i - \varepsilon) \qquad (3)$$

The voltage jump occuring at t_i is then given by :

$$\sigma_i = V(t_i - \varepsilon) - V(t_i + \varepsilon) = V_l(t_i - \varepsilon) + V_c(Z_{i-1}) - V_c(Z_i) \qquad (4)$$

The arc voltage can also be defined by using the voltage drop along the arc column, $V_c(Z)$.

It comes, following fig 3 :

$$V(t) = U_c + V_c(Z) + V_g(Z, t) \qquad (5)$$

Introduicing eq. (1) in eq. (5) for $t_{i-1} < t < t_i$, gives the voltage between the column and the anode wall :

$$V_g(Z, t) = U_a + V_c(Z_{i-1}) + V_l(t) - V_c(z) \qquad (6)$$

If $V_g(Z, t)$ becomes higher than a given value, $V_b(Z)$, depending on the cold layer thickness e(Z), the arc restrikes to another location giving rise to a new spot at Z_i. This situation is represented schematically in figure 4 where the shaded area corresponds to $V_g(Z, t) \geq V_b(Z)$. From this figure, it can be seen that the vertical coordinate at $Z = Z_i$, that is $V_b(Z_i)$, is such that :

$$V_g(Z_i, t_{i-\varepsilon}) = V_b(Z_i) = \sigma_i + U_a \qquad (7)$$

The voltage breakdown $V_b(Z)$ is related to the thickness e(Z) of the cold layer following the relationship :

$$V_b(Z) = E_b . e(Z) \qquad (8)$$

where E_b is the breakdown field for which no reliable values are available concerning these specific experimental situations. As suggested in figure 4, the breakdown voltage increases in the upstream direction due to the

thickner cold layer in the vicinity of the cathode tip. That means that the highest values for the jumps must be obtained for the breakdowns occuring close to the cathode.

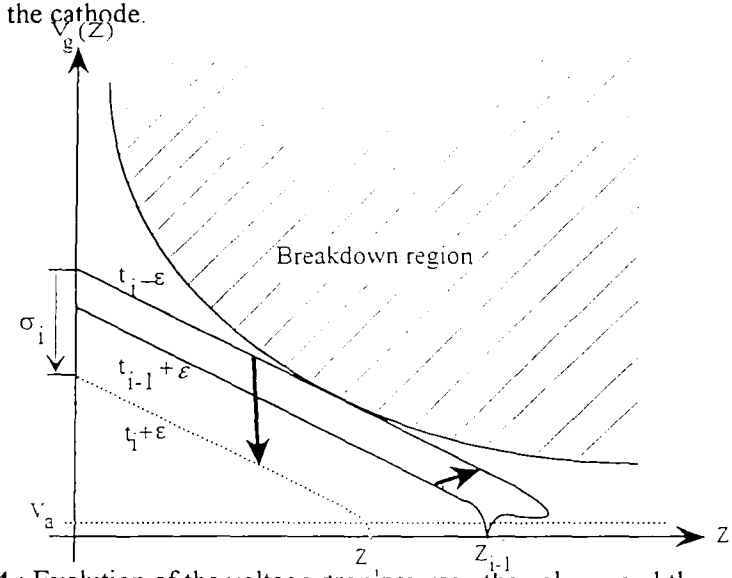

Figure 4 : Evolution of the voltage drop between the column and the anode wall.

In the ideal case where the arc column shows a well defined, axisymetric and stable configuration, the breakdown region is limited by a monotonous decreasing curve such as the one plotted in fig. 4. In the real case where, for example, turbulence takes place, the frontier of the shaded area can only be defined as a mean curve. In addition, for the situations corresponding to the downstream restrikings, the limiting curve must be represented by a multi-branched and time dependent function rather than a single valued one.

Nevertheless, the previous considerations have been qualitatively verified by plotting the voltage jump amplitudes versus their corresponding voltage minima. As an example, fig. 5-a and 5-b show the results obtained for the plasma torch equipped with a nozzle 8 mm in diameter, operated with a 45/15 slm Ar/H2 mixture and a 609 A current intensity. About one thousand upstream jumps are plotted in fig. 5-a, which define a rather well pronounced tendency around a decreasing curve.

Fig. 5-b is related to the downstream restrikings, where the events clearly separate into two groups of points, the highest one being

qualitatively attributed to the B situation in the fig. 1 instead of the C situation for the lowest group.

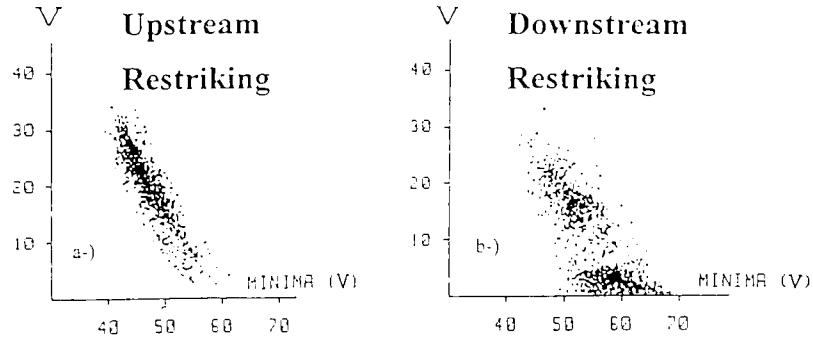

Figure 5 : Individual voltage jumps versus their corresponding voltage minima
a -Upstream restriking. b - Downstream restriking.

The distributions of the spot lifetimes versus the corresponding voltage minima are presented in fig. 6-a and 6-b for the upstream and the downstream restrikings respectively. It can be seen on both figures that the highest lifetimes are those of the spots corresponding to the lowest voltage minima. The lifetimes correponding to the downstream restrikings roughly separate into two groups in the same way than for the jump amplitudes. The fact that the highest lifetimes are obtained for the lowest voltage minima is an interesting finding because of its implication on the erosion mechanism understanding. That means that the erosion is enhanced in the regions corresponding to a short arc column, as it was qualitatively confirmed by the wear of the anode material.

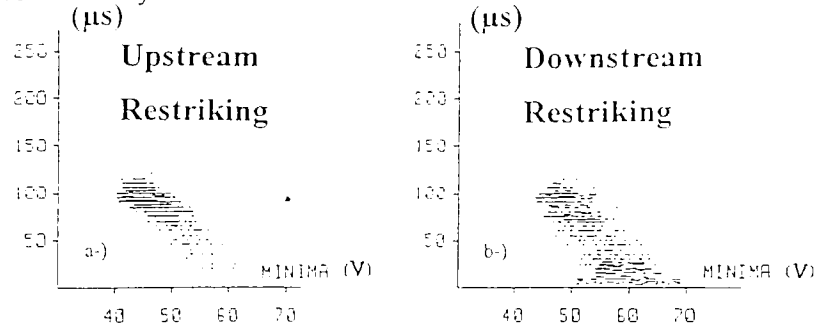

Figure 6 : Individual spot lifetimes versus their corresponding voltage minima
a -Upstream restriking. b - Downstream restriking.

4. GENERAL TENDENCIES

The operating conditions were changed in order to bring out the influence of the arc current intensity, nozzle diameter or gas flowrate on the arc dynamic. As mentioned in the previous section, the cold layer thickness plays a crucial role for both the jump amplitudes and the spot lifetimes. This thickness is determined by the radius of the nozzle channel and by the radius of the arc, which increases with the current intensity. The effect of the arc current increase is illustrated in fig.7 where the probability distributions of the voltage jump amplitudes are plotted, disregarding the "upstream" and "downstream" cases. It can be noted that for the lowest value of the arc current, the small jumps are almost absent. The "hole" in the distribution is progressively filled when the current is raised, testifying of a modification of the distribution shape rather than a shift of the range of the voltage jumps. This modification is however accompanied by a monotonic decrease of the voltage jumps mean value, $\overline{\sigma}$.

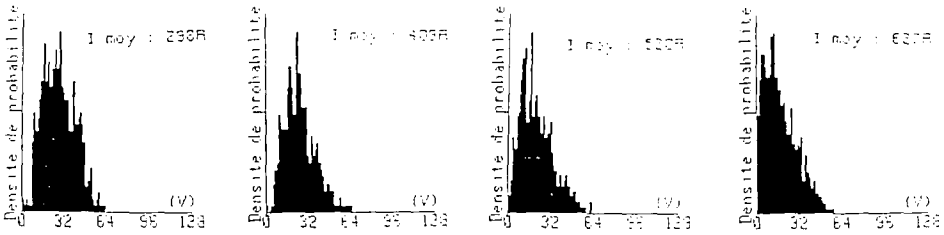

Figure 7 : Probability distributions of the voltage jump amplitudes versus the arc current intensity.

The same tendencies were observed at constant current by changing the nozzle diameter so that a larger diameter was qualitatively equivalent to a smaller arc current. The corresponding results are presented in fig.8, representing the jump mean values evolution with the arc current, for different nozzle diameters and for a single gas flowrate corresponding to an Ar/H2 mixture (45/15 slm respectively).

A well defined tendency was also found for the anodic spot lifetimes, $\overline{\tau}$, where mean values are plotted in fig.9 for different operating conditions. The similarity of the evolutions of both $\overline{\sigma}$ and $\overline{\tau}$ as it can be noted in fig.8 and 9 is due to the fact that the small jumps occur when there is not time enough for the arc to be significantly lengthened, that is to say,

when the spots are more frequently created. This is the case when the cold layer which surrounds the arc is thin, allowing all the perturbations in the fringes, despite their size, to give rise to a breakdown. When using a small nozzle diameter, the thickness of the cold layer significantly decreases when the current increases in contrast with a 10 mm nozzle diameter for which the cold layer remains thick whatever the arc current is (at least in the studied range i.e. below 650 A). In that last case, only the strongest perturbations in the fringes, that is the less frequent ones, can lead to breakdowns associated with large jump amplitudes and long lived spots.

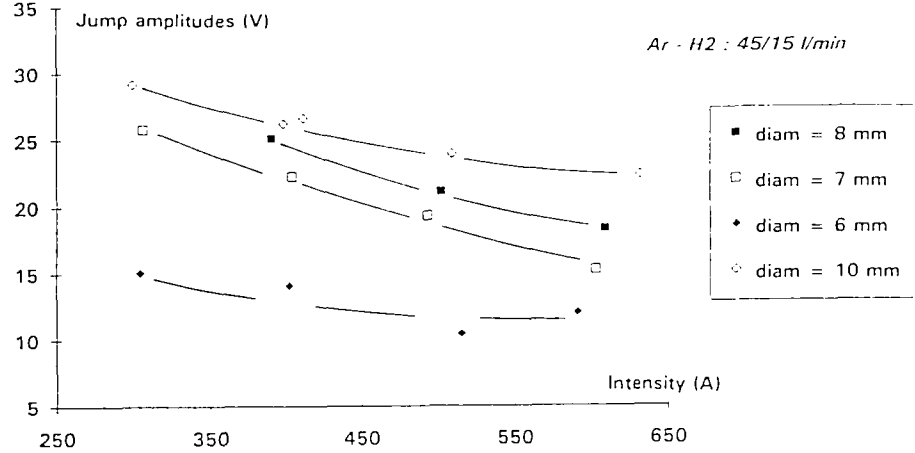

Figure 8 : Evolution of the mean jumps with the arc current, for different nozzle diameters.

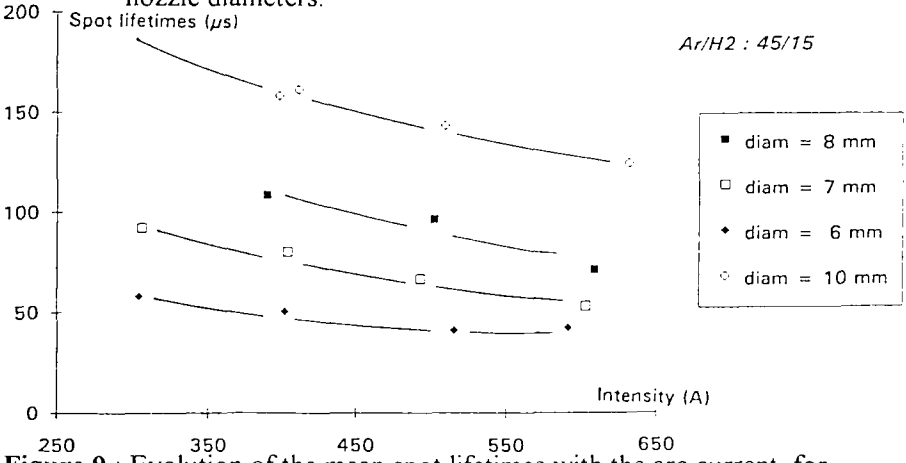

Figure 9 : Evolution of the mean spot lifetimes with the arc current, for different nozzle diameters.

The gas mass flowrate seemed to have a double role because, on the one hand, it determined the rate at which the arc was stretched, and on the other hand, it influenced the tubulence and the occurence of the perturbation in the arc column fringes. This was qualitatively confirmed by the fact that an increase of the mass flowrate provoked a significant increase of the mean voltage jump, $\bar{\sigma}$ and, to a lesser extent a decrease of the anodic spot lifetime $\bar{\tau}$.

By using dimensional analysis together with correlations between relevant dimensionless groups, it was found [9] that the spot lifetimes changed with the operating parameters according to the approximate formula :

$$\bar{\tau} \approx K. \frac{D^2}{(G.I^2)^{\frac{1}{3}}}$$

where K depended on the gas nature (N2 or Ar/H2).

Furthemore, by distinguishing between the upstream and the downstream rearcing, it was systematically found that the "upstream" spot lifetimes are about 30-40 % higher than the "downstream" ones. This difference may have a considerable importance, namely in the case where the spot lifetime must overcome a time threshold for initiating the local erosion.

5. ESTIMATION OF THE MEAN ARC-ROOT POSITION

A tentative analysis was made to estimate both the arc-root position at the nozzle surface and the mean electric field in the arc column. The basic idea to carry out these measurements was suggested by the strong similarities observed between the arc-voltage waveform and the signal resulting from the optical sampling of the luminosity emitted by the plasma jet at the nozzle exit. As illustrated in fig. 10-a, a plasma "bubble" was disconnected from the arc column each time a restrike occured.

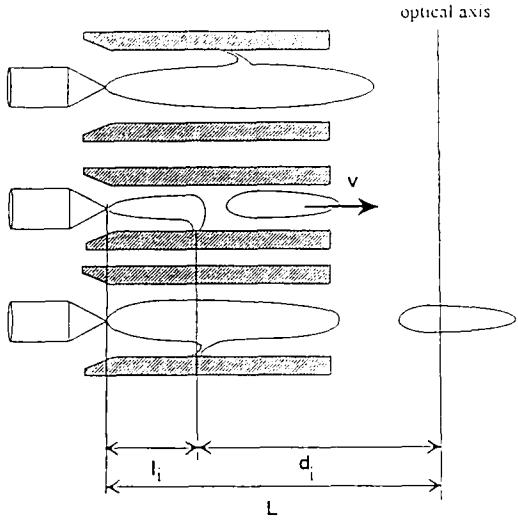

Figure 10 : Estimation of the arc-root position at the nozzle surface and the mean electric field in the arc column.

The "extinguishing" plasma bubble was then travelling in the flow direction with a given velocity, v (fig. 10-b), and crossed the line of sight of an optical system which comprised a focusing lens, an optical fiber and a photomultiplier connected with a digital oscilloscope [10].

When a bright plasma bubble crossed the optical axis, it generated a peak which could be clearly associated with a corresponding detail in the voltage signal as illustrated in fig. 11.

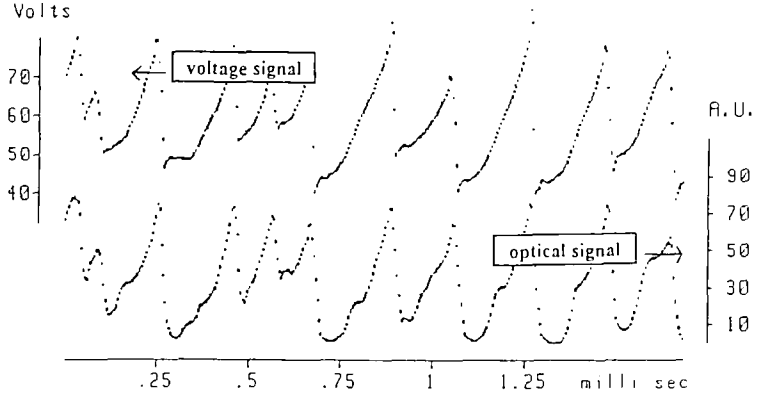

Figure 11 : Voltage and optical signals.

More precisely, each voltage jump corresponded to a local delay of the optical signal, associated to the back front of a flying plasma bubble. For each of them, a delay, θ_i, between the corresponding voltage jump and the "optical jump" was estimated. This delay, θ_i, was believed to correspond to the time of flight of the plasma bubble from the place where the arc restriked at time t_i, to the optical axis position reached by the back front of the bubble at time $t_i + \theta_i$. Following the indication of the fig. 10, it comes :

$$\theta_i = \frac{d_i}{v} = \frac{L - l_i}{v} \qquad (10)$$

where v is the flow velocity assumed to be constant. L is the known distance between the cathode tip and the optical axis, l_i is the length of the arc column immediately after the restriking. This arc length, l_i, corresponds to a voltage local minimum, $V_m(t_i)$, so that :

$$V_m(t_i) = U_a + U_c + E.l_i \qquad (11)$$

where U_a and U_c are the anodic and cathodic falls, and where E is the mean electric field in the arc column.

Introducing eq. (11) in eq. (10), it comes for the individual delay,

$$\theta_i = \frac{L}{v} - \frac{V_m(t_i) - U_a - U_c}{E.v} \qquad (12)$$

It has to be noted that the time which characterized the sharp decreases, or jumps, in both signals are different. For this reason, the choice was made for a definition of the delay, as the difference between the mid height of the corresponding two optical and electrical signals.

Following eq (12), the evolution of the individual delays, θ_i, with their corresponding voltage minima, $V_m(t_i)$, must fall on a straight line from which both the velocity, v, and the electric field, E, can be deduced.

The anodic and cathodic falls were respectively estimated to be U_a=15 and U_c=5 Volts and the distance L was 30 mm.

The results obtained with a 8 mm nozzle diameter, a 204 A current and a 45/15 slm Ar/H2 flowrate are presented in fig. 12 where a few hundreds of data points are gathering around the linear evolution predicted by eq (12).

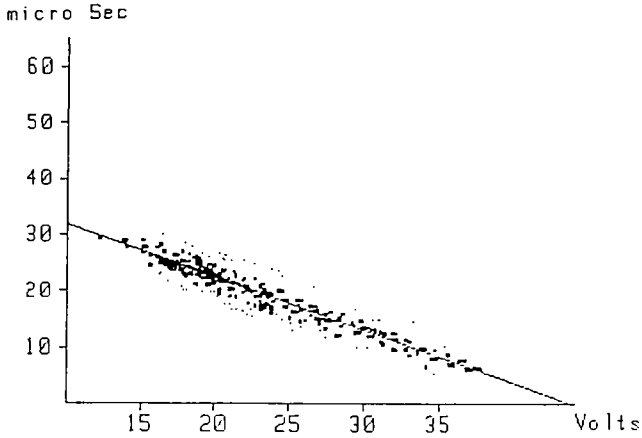

Figure 12 : Evolution of the individual delays versus their corresponding voltage minima.

The intercept of the linear adjustement and vertical axis gave 730 m/s for the velocity which was in very good agreement with the value obtained independantly by a specific measurement technique [10]. The mean electric field, deduced from the slope of the plot was estimated to be 1450 V/m in that case.

In addition, from the voltage minima $V_m(t_i)$ and using eq (11) together with the value previously obtained for the electric field, allowed us to evaluate the position of the arc root defined as the mean value, $\bar{l}$, of the distances, l_i, measured from the cathode. Assuming the erosion to be enhanced by the stagnation time of the spot at the surface, $\bar{l}$ was identified to be the mean location of the wear, provided it was calculated by using the following weighted mean :

$$\bar{l} = \frac{\sum_{i=1}^{N} l_i \cdot \tau_i}{\sum_{i=1}^{N} \tau_i} \qquad (13)$$

where N is the number of restrikings identified during the signals recording (a few hundreds). For the experiment corresponding to the fig. 12, it was found : $\bar{l} \approx 17$ mm.

The torch was operated under different conditions so that the tendancies shown by the electric field, $\bar{\mathcal{E}}$, and by the position of the wear at

the nozzle wall were brought out. It was found that $\bar{\mathcal{E}}$ slightly increases when the current increases or when the nozzle diameter decreases. For example, the measurements obtained for a 8 mm nozzle diameter gave a variation of $\bar{\mathcal{E}}$ from 1450 to 1950 V/m when the current changed from 200 to 630 A. In the case of a 10 mm nozzle diameter, the same tendancy was observed for the same current range, with a field change from 1300 to 1800 V/m.

The tendancies shown by the mean location of the wear, calculated using eq. 13, were also rather defined. Increasing the arc current or decreasing the diameter made the erosion to occur closer to the cathode tip. For example, $\bar{l}$ changed from 22 to 18 mm when the current increased from 200 to 630 A, in the case of a 10 mm nozzle diameter, and from the 17 to 13 mm for the same current range but with a 8 mm nozzle diameter.

These results obtained for the mean position of the erosion corresponded qualitatively with the examination after each run of the wear traces left in the nozzle.

It was also surprising to find that the wear was closer to the nozzle exit when using a larger nozzle diameter, in contrast with what would be thought, taking only into account the effect of the flow velocity. This situation confirms the importance of the electrical breakdowns through the insulating cold layer which surrounds the arc and which thickness plays a role of prime importance for the dynamic equilibrium of the arc.

6. CONCLUSION

A detailed analysis of the arc voltage fluctuations has revealed interesting features concerning the constricted arc dynamic. The shape of the details observed in the time resolved voltage waveform seemed to be strongly correlated to the arc instantaneous morphology, which evolution determined the plasma flow structure and temporal behavior. Simultaneous measurements of the arc voltage and of the radiation intensity emitted by the plasma were carried out. The similarities observed between the signals have suggested the mechanisms involved in the creation of the plasma flow which appeared to be rather a heterogeneous medium, made of flying and extinguisling plasma bubbles, surrounded by colder layers. An in situ method was developed for the electric field measurement together with the determination of the position of the erosion inside the nozzle. The results obtained with this new method indicate that the study of the fluctuating

component of the relevant plasma torch parameter could lead to new diagnostic techniques.

REFERENCES

[1] S. VACQUIE, in "L'arc électrique et ses applications" , Tome 1, p. 135, (1984),
Ed CNRS, Paris

[2] S. PAIK, P.C. HUANG, J. HEBERLEIN and E. PFENDER, Plasma Chemistry Plasma Processing, 13 (3), p. 379-397, (1993)

[3] S.A. WUTZKE, E. PFENDER and E.R.G. ECKERT, AIAA J. (6) 8, p.1474, (1968)

[4] W. NEUMANN, Beitr. Plasma Physik, 16, p.97, (1976)

[5] M.F. ZHUKOV, "Electrical arc plasmatrons", edited by the USSR Academy of Sciences, 630090 Novossibirsk - 90 - (Pub) Esperanza engineering group (1977)

[6] H.H. MAECKER and H.G. STABLEIN, in IEEE Transactions Plasma Science, Vol. PS - 14, n°4, p. 291, (1986)

[7] T.S. CHOU, E. PFENDER, in Wärme und Stoffübertragung 6, p. 69-77. Springer-Verlag (1973)

[8] H.A. STINE and V.R. WATSON, NASA TN D-1331 (1962)

[9] J.F. COUDERT, M.P. PLANCHE, P. FAUCHAIS, in High Temp. Chem. Processes 3 (6), p. 639-652, (1995)

[10] J.F. COUDERT, M.P. PLANCHE, P. FAUCHAIS, in Plasma Chemistry Plasma Processing 15 (1), p. 47-70, (1995)